Supporting Information

to

Direct Synthesis of Inverse Hexagonally Ordered Diblock Copolymer/ Polyoxometalate Nanocomposite Films

Thomas Lunkenbein,[†] Marleen Kamperman,[‡,] Zihui Li,[∥] Carina Bojer,[†] Markus Drechsler,[§] Stephan Förster,[⊥] Ulrich Wiesner,[∥] Axel H.E. Müller,[§] and Josef Breu[†,*]*

[†]Inorganic Chemistry I, [§]Macromolecular Chemistry II and [⊥]Physical Chemistry I, University of Bayreuth, 95440 Bayreuth, Germany; [‡]Physical Chemistry and Colloid Science Wageningen University, 6703 HB Wageningen, Netherlands; [∥]Materials Science & Engineering Cornell University Ithaca, NY 14853, USA

I. Pre-treatment of Molybdophosphoric acid ($H_3[PMo_{12}O_{40}]$, H_3PMo)

Heteropoly acids (HPA) tend to change their degree of hydration and therefore their crystal structure depending on the relative humidity (RH).[1] In order to generate a defined and reproducible stoichmetry of the H_3PMo precursor, the Keggin was recrystallized from water. Thermogravimetric analysis (TGA) shows the presence of 27 H_2O molecules per formula unit (see Figure SI 1).

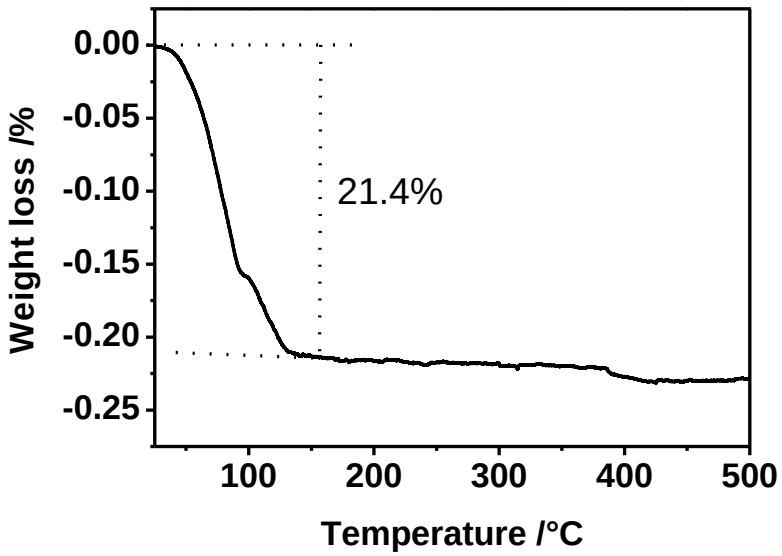

Figure SI 1: TGA measurements of H_3PMo recrystallized from water and stored 86 % RH. Evaluation of the mass loss equals the loss of 27 water molecules per H_3PMo unit.

II. Film casting reactor.

Well-ordered poly(butadiene-block-2-dimethylaminethyl methacrylate) (PB-b-PDMAEMA) mesostructures were observed when the solvent was allowed to evaporate at 32 % RH. Hence, we engineered a film casting reactor to adjust the desired RH (see Figure SI 2). It is known that a defined RH adjusts above a saturated salt solution in solution. In our case a saturated $CaCl_2$ yields 32 % RH. An aquarium pump delivers the moisturized air into the reactor. After equilibration, volatiles are allowed to evaporate.

Figure SI 2: Photograph of the self-built film casting reactor.

III. Calculation of the Florry-Huggins interaction parameter χ

The Florry-Huggins interaction parameter χ represents the quality of a solvent to dissolve a polymer and can be calculated as follows:

$$\chi = \frac{V_M}{RT}\left(\delta_{polymer} - \delta_{solvent}\right)^2 \qquad \text{I}$$

where V_M is molar volume, R represents the ideal gas constant (1.9 calJK^{-1}mol^{-1}), T is the casting temperature (T=298 K) and δ is solubility parameter. The values of V_M and δ values are given in Table SI 1:

Table SI 1: Molar volume V_M and solubility parameter δ of PB, PDMAEMA, THF and acetone.

polymer	solvent	V_M /cm^{3}mol^{-1}	δ /(calcm^{-3})$^{0.5}$
PB		58.85[2]	8.05[2]
PDMAEMA		136.17	9.21[2]
	THF		9.1[2]
	acetone		9.9[2]

IV. Colloidal Solution

In order to check the stability of the solution even at higher concentration and high loadings, photographs were taken at different states of evaporation and the corresponding concentration was calculated. The inorganic H_3PMo loading was 83 wt % with respect to the amount of diblock copolymer. The corresponding photographs are depicted in Figure SI 3. For the sake of clarity glass vials were taken instead of the TEFLON dishes.

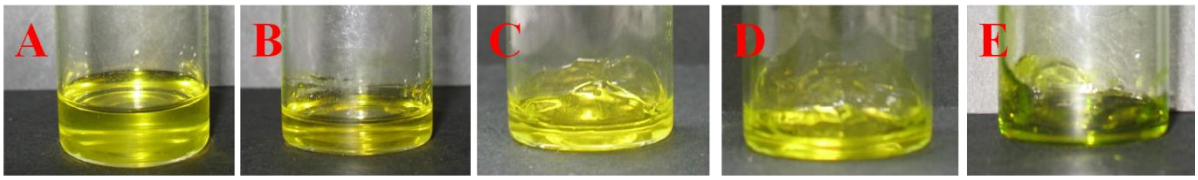

Figure SI 3: Photographs of PB-b-PDMAEMA/H_3PMo solution in THF (H_3PMo loading: 83 wt % with respect to the diblock copolymer) at different states of evaporation and concentration: A) initial solution (13 wt %), B) 28 wt %, C) 40 wt %, D) 69 wt % and E) 90 wt %.

The presence of colloids in solution was proven by a simple laser experiment (λ= ~540 nm). A solution of PB-b-DMAEMA/H_3PMo (70 wt % H_3PMo) was irradiated by a laser. The photograph in Figure SI 4 clearly shows Tyndall scattering, originating from PB-b-PDMAEMA/H_3PMo complexes in THF solution.

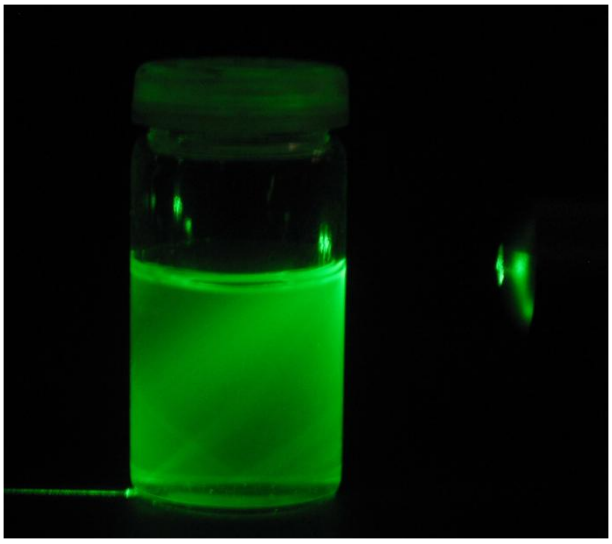

Figure SI 4: Photograph of PB-b-PDMAEMA/H_3PMo complex in solution (70 wt % H_3PMo) irradiated by a laser.

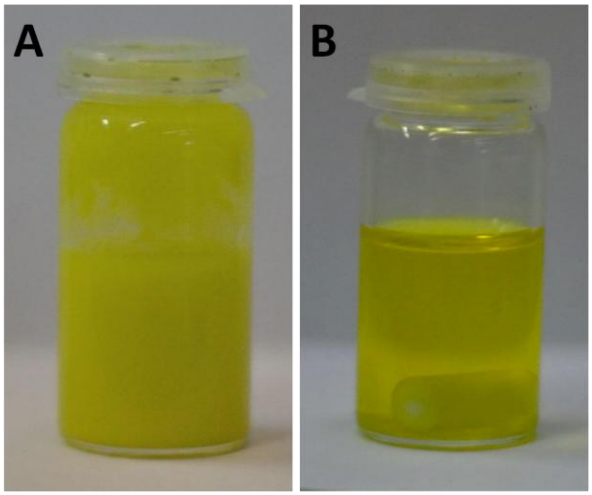

Figure SI 5: Images of ionizable diblock copolymers/H_3PMo solutions with varying degree of polymerization: A) PB_{288}-b-$PDMAEMA_{244}$ and B) PB_{476}-b-$P2VP_{126.}$ The indices denote the degree of polymerization. In all cases the concentration was 80 g/L and the H_3PMo content was 70 wt %.

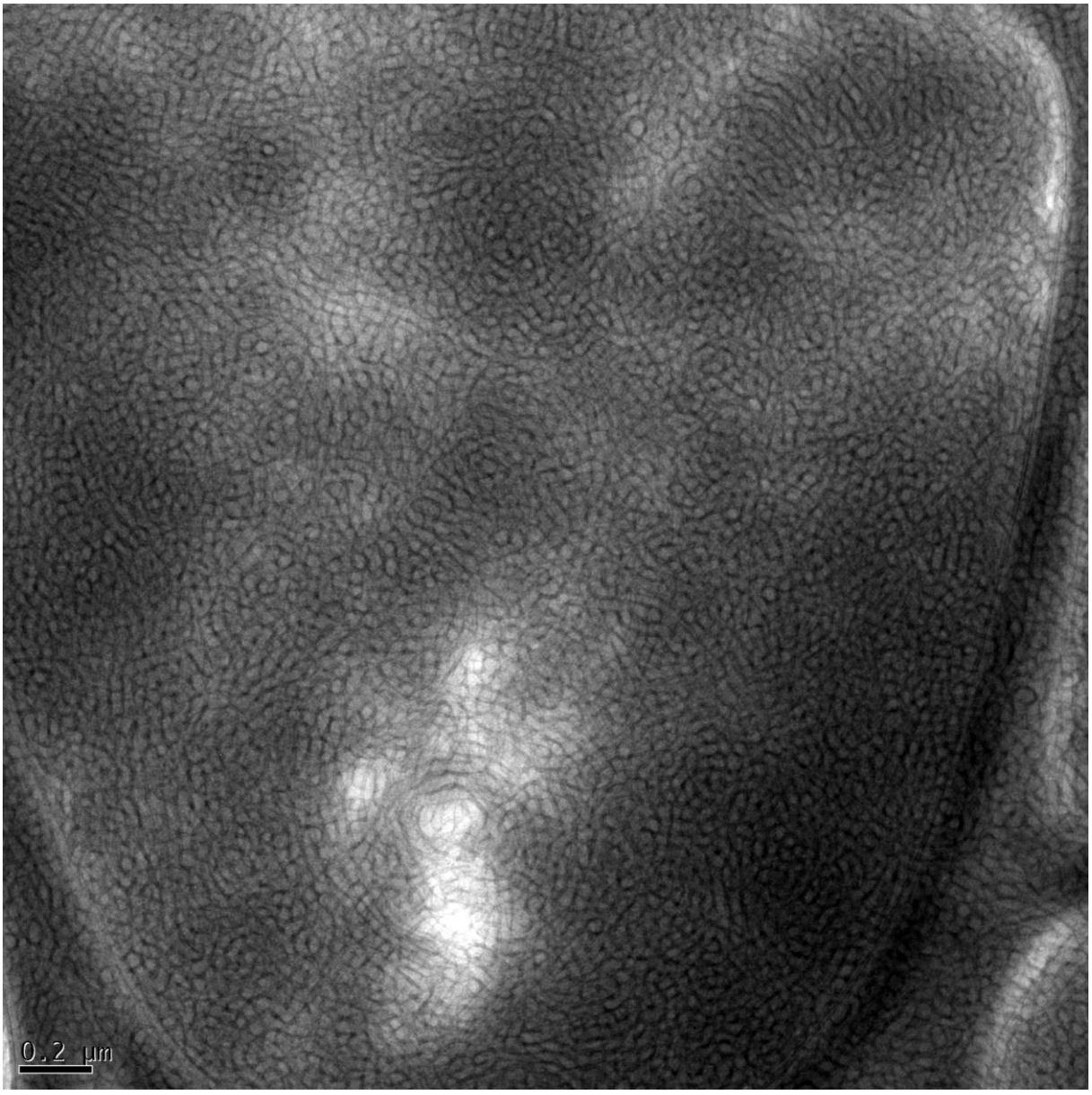

Figure SI 6: Cryo-TEM of 3D bicontinuous network vitrified in THF.

V. DLS measurements

Although high concentrations of up to 115 g/L (where the transition occurs) will induce multiple light scattering and might hamper Brownian motion due to particle interactions dynamic light scattering was measured (Figure SI 7). While the absolute values are expected to be in error, the trends in morphology transitions could nevertheless be seen. Figure SI 7 A to C show the auto correlation curves obtained for PB-b-PDMAEMA/H3PMo ratio of 3.23, 1.08, and 0.54, respectively. Please note, that for the latter the angle at 30° was neglected since multiple measurements were not reproducible. The results obtained for Γ versus q^2 (Figure SI 7 D) and Γq^{-2} versus q^2 (Figure SI 7 E) follow the trend seen by cryo-TEM measurements.

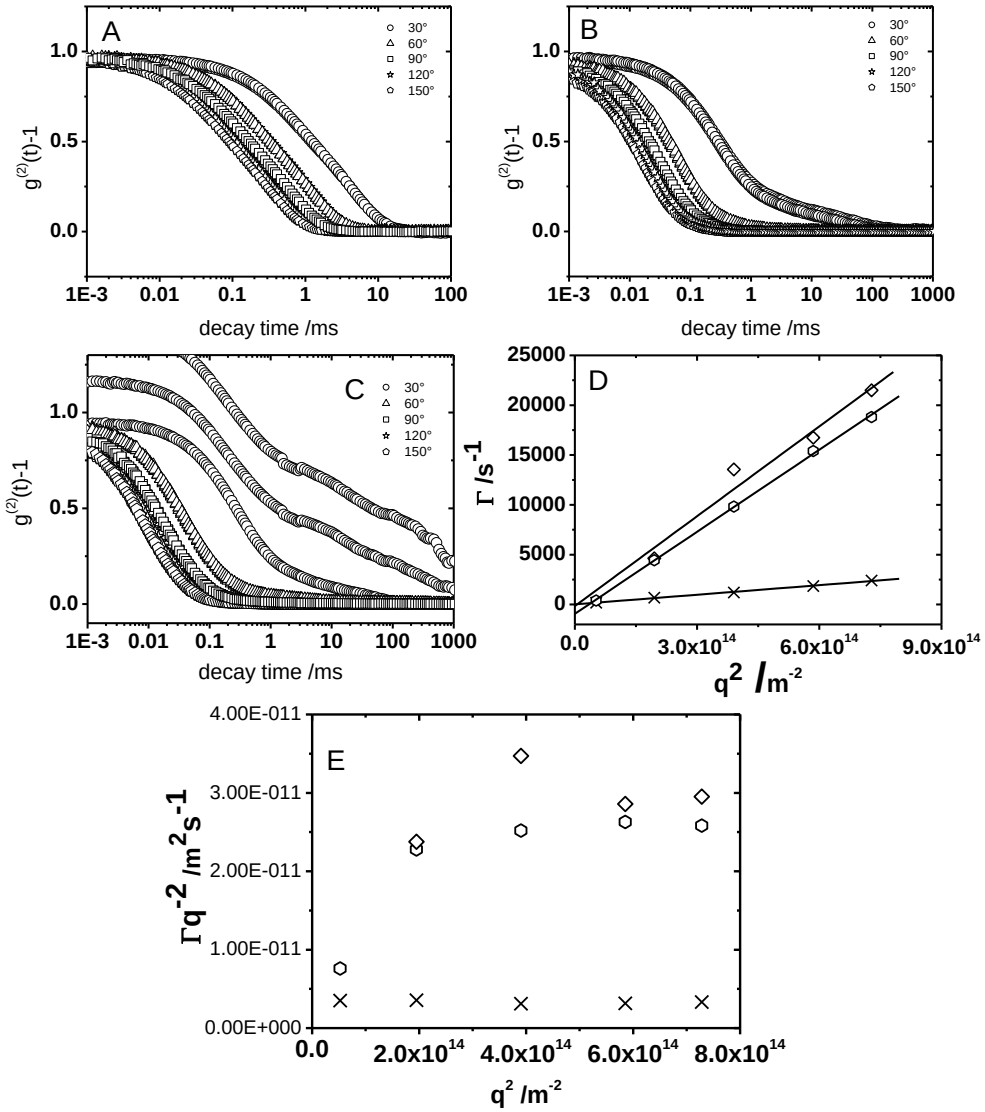

Figure SI 7: DLS measurements of different PB-b-PDMAEMA/H_3PMo complexes. A) to C) auto correlation curves of samples exhibiting a PB-b-PDMAEMA to H_3PMo ratio of 3.23, 1.08, and 0.54, respectively at different angles: ○ 30°, Δ 60°, □ 90° ☆ 120°, and ⌂ 150°. D) q dependence of the experimental relaxation rate and E) q dependence of the translational diffusion coefficient for different PB-b-PDMAEMA to H_3PMo ratios: × 3.23, ⬡ 1.08, and ◇ 0.54.

VI. Calculation of the packing parameter

$$V_{PB} = \frac{M_{PB}}{N_A \rho_{PB}} \qquad II$$

$$V_{PDMAEMA} = \frac{M_{PDMAEMA}}{N_A \rho_{PDMAEMA}} \qquad III$$

$$f_{PDMAEMA} = \frac{V_{PDMAEMA}}{V_{PB} + V_{PDMAEMA}} \qquad IV$$

$$V_S = V_{PDMAEMA} + 40\frac{V_{POM}}{r} \qquad V$$

$$f_{S,calc} = \frac{V_S}{V_S + V_{PB}} \qquad VI$$

$$f_{S,TEM} = \frac{\frac{\sqrt{3}}{2}(A+B)^2 - \left(\frac{1}{2}\cdot B\right)^2 \cdot \pi}{\frac{\sqrt{3}}{2}(A+B)^2} \qquad VII$$

$$S_c = \frac{d_c}{2L_{PDMAEMA}} \qquad VIII$$

Here V, M ,ρ and f are the volume, molecular mass, density and volume fraction of the corresponding block denoted by subscripts, respectively. N_A is the Avogadro number (N_A=6.022*10^{23} mol^{-1}). V_s represents the solvophobic volume and $f_{s,calc}$ denotes the calculated theoretical volume fraction of the solvophobic block. $f_{s,TEM}$ is the calculated solvophobic volume based on the dimensions of the PB block (A) and PDMAEMA/H_3PMo matrix (B) obtained from TEM images. V_{POM} is calculated by the knowledge of the anionic radius of H_3PMo (V_{H3PMo} = 0.596 nm^3) and tungtophosphoric acid (H_3PW, V_{H3PW}=0.599 nm^3).[3] S_c shows the stretching degree of the core block in THF solution. It is directly proportional to the core diameter, d_c, in solution. L indicates the contour length (L=DP*0.25 nm) where DP is the degree of polymerization of the PDMAEMA block.

Table SI 2: Characteristic values of the different diblock copolymers considered for the calculation of the packing parameters.

diblock copolymer	block	M /gmol^{-1}	ρ /gcm^{-3}	DP
PB-b-PDMAEMA	PB	22620	0.902[4]	418
	PDMAEMA	6380	1.318[5]	40
PB-b-P2VP	PB	22200	0.902[4]	411
	P2VP	7800	1.145[2]	75

VII. Affinity of THF to H_3PMo

The following experiment was conducted in order to study the high affinity of H_3PMo crystals to adsorb THF. 300 mg of recrystallized H_3PMo were placed separately from 3 mL distilled THF in an exsiccator as depicted in Figure SI8 A and B. The closed system was allowed to equilibrate for 30 min. During this time the H_3PMo starts to liquefy upon adsorbing of gaseous THF (see Figure SI 8 C and D). The very high adsorbing affinity tends to break up lattice energy and dissolves the H_3PMo in THF.

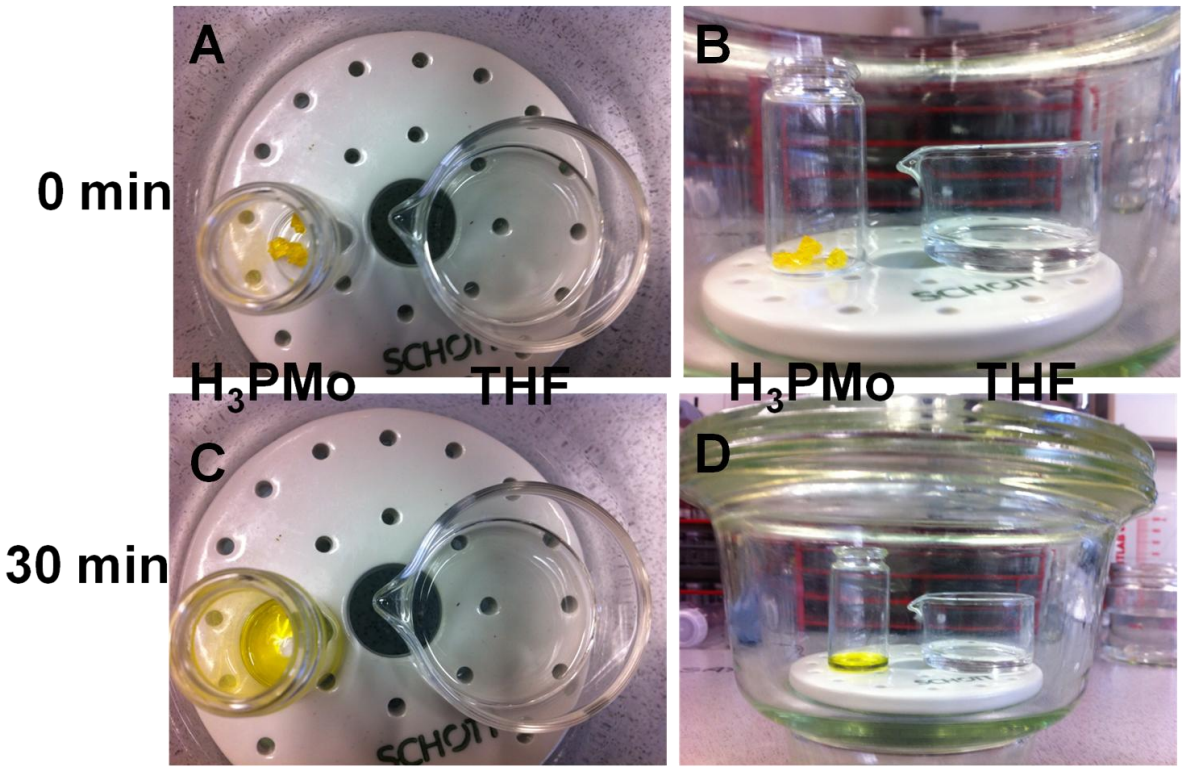

Figure SI 8: Visualization of the high affinity of H_3PMo to adsorb THF. A) and B) show the initial state with solid H_3PMo, whereas C) and D) represent the H_3PMo/THF system after allowing to equilibrate for 30 min. in an exiccator. The liquefaction of the H_3PMo crystals is clearly observable.

To further proof the strong adsorption of THF over H_3PMo two ^{1}H-NMR experiments in d^6-acetone were conducted (see Figure SI 9). In Figure SI 9A pristine recrystallized H_3PMo was directly dissolved in d^6-acetone. The blue arrows denote the hydrogen bonding to bridge oxygen (δ=2.10 ppm) and to terminal oxygen (δ=5.32 ppm), respectively.[6] After film casting from THF and re-dissolving in d^6-acetone these peaks are gone, but a new triplette arises at δ =3.64 ppm and a quintette arises at δ =1.80 ppm, corresponding to THF.

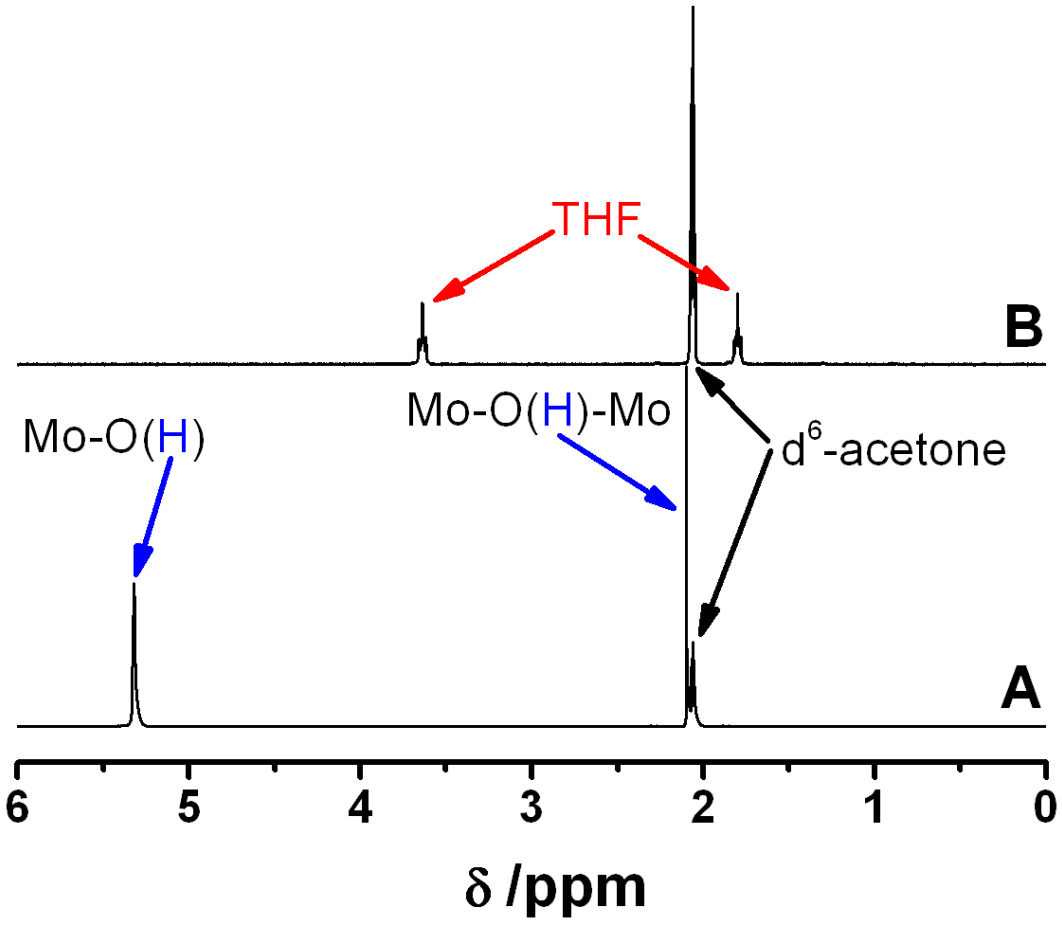

Figure SI 9: ^{1}H-NMR spectra of A) pristine H_3PMo in d^6-acetone and B) after H_3PMo film casting from THF and re-dissolution in d^6-acetone.

VIII. FTIR and PXRD

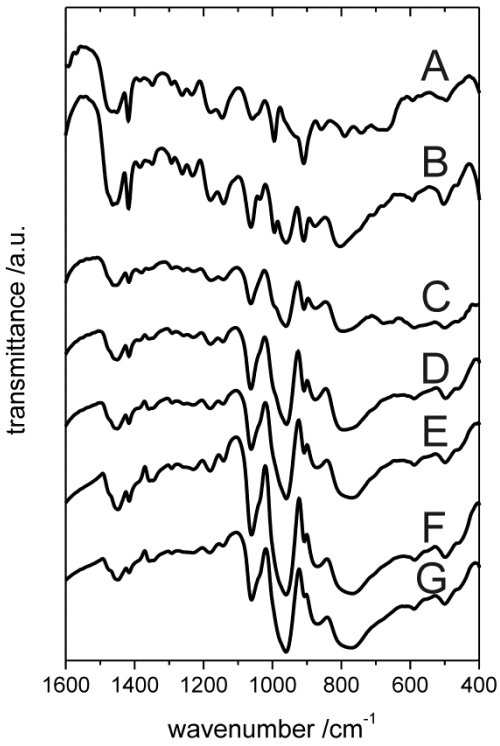

Figure SI 10: FTIR- spectra of PB-b-PDMAEMA/H_3PMo nanocomposites with different H_3PMo loading A) 28 wt %, B) 44 wt %, C) 61 wt %, D) 70 wt %, E) 76 wt %, F) 80 wt %, and G) 83 wt %.

Table SI3: Characteristic asymmetric vibrations of the four different oxygen bonds in H_3PMo obtained from FTIR spectra of the different composite films.

	υ_{as} (P-O_a)	υ_{as} (Mo-O_b)	υ_{as} (Mo-O_c-Mo)	υ_{as} (Mo-O_d-Mo)
Reference[7]	1064	962	869	787
H_3PMo	1064	960	869	784
1:0.5	1061	952 (sh)	858	790
1:1	1062	960	877	804
1:2	1063	961	875	794
1:3	1063	959	876	794
1:4	1062	960	871	770
1:5	1061	960	869	768
1:6	1061	961	869	771

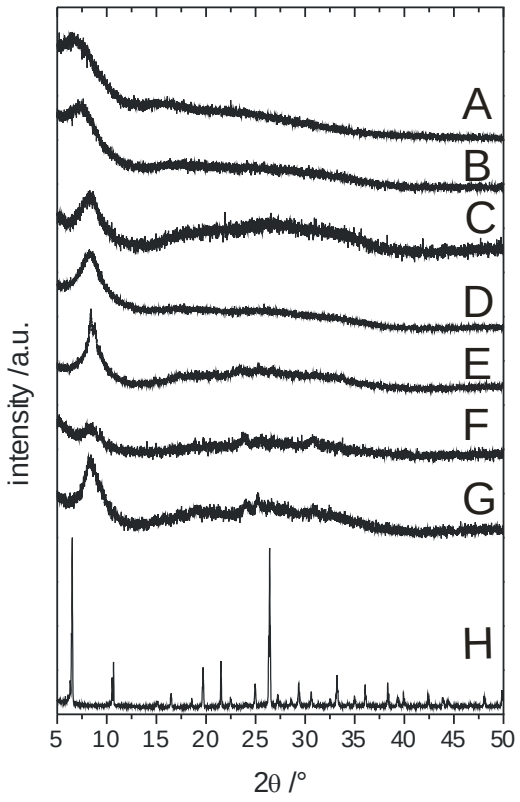

Figure SI 11: PXRD patterns of PB-b-PDMAEMA/H_3PMo nanocomposites with different H_3PMo loading: A) 28 wt %, B) 44 wt %, C) 61 wt %, D) 70 wt %, E) 76 wt %, F) 80 wt %, G) 83 wt %, and H) parent H_3PMo.

IX. Mesophase behavior

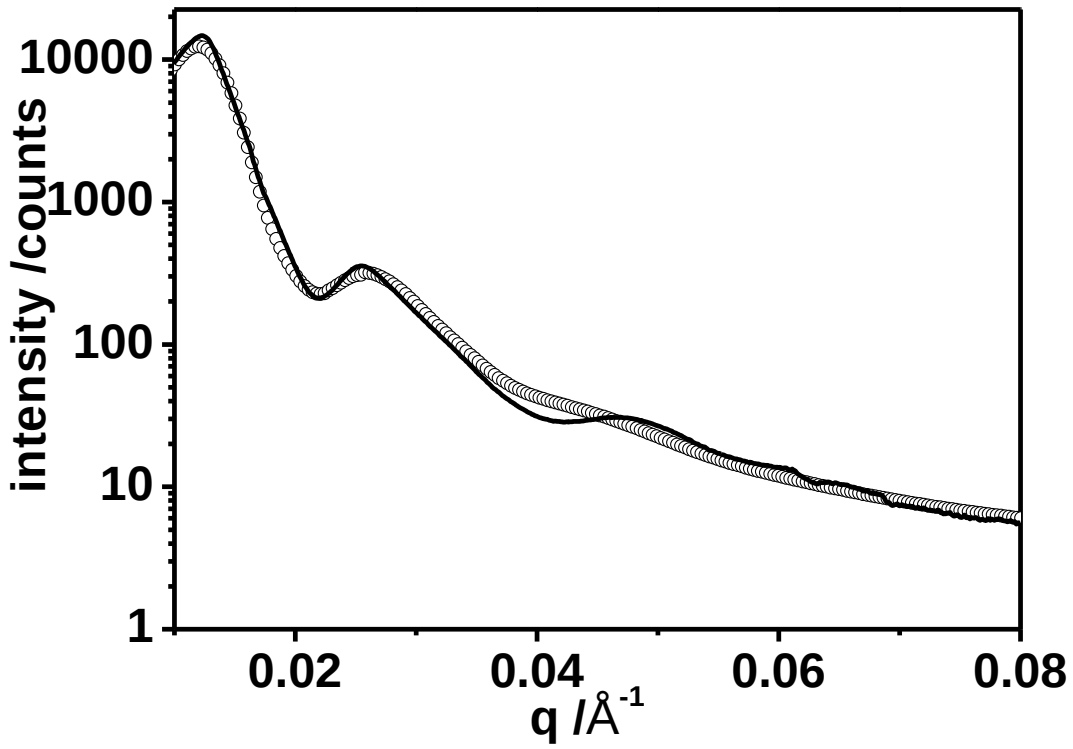

Figure SI 12: SAXS traces of PB-b-PDMAEMA/H_3PMo with H_3PMo loading of 76 wt %. The dotted line denotes a fit to a hexagonal lattice. Pleas note, that the absence of the √3 reflex in the SAXS pattern is due to a minimum of the cylinder form factor at this position.

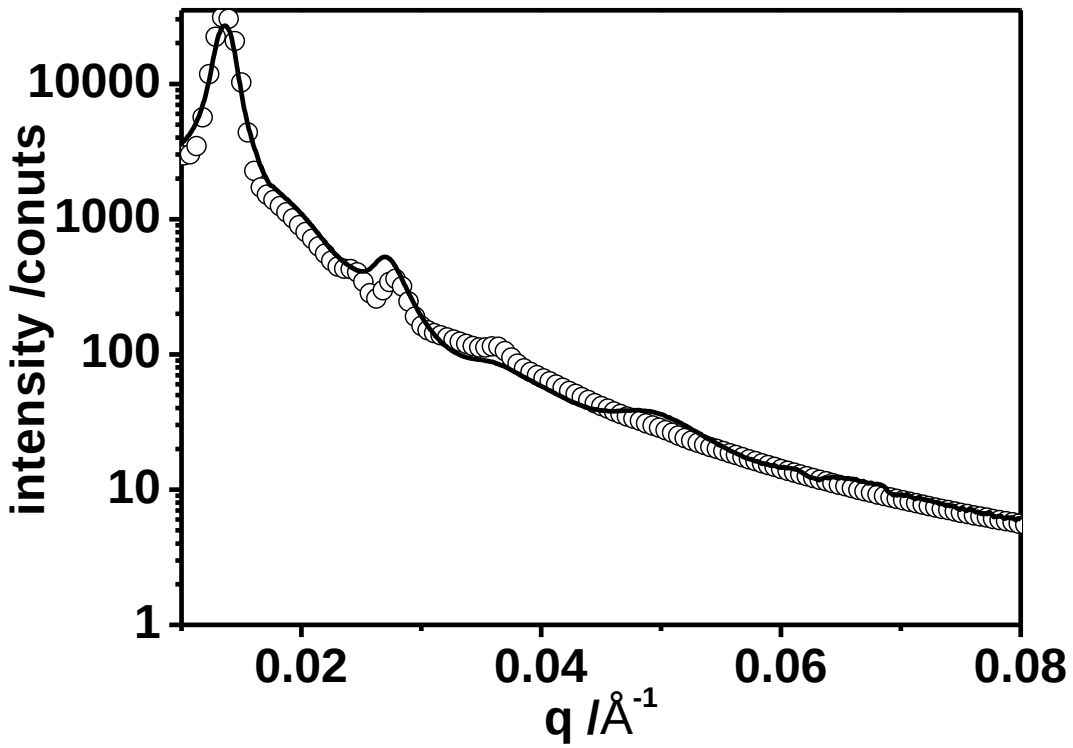

Figure SI 13: SAXS traces of PB-b-PDMAEMA/H_3PMo with H_3PMo loading of 80 wt %. The dots denote a fit to a hexagonal lattice.

X. Genarlization

In order to show that our approach towards inverse hexagonal PB-b-PDMAEMA/H_3PMo nanocomposites is a more general approach, two additional experiments were conducted. First, PB-b-P2VP was used as ionizable diblock copolymer instead of PB-b-PDMAEMA. The SAXS and TEM results below on the resulting composites (Figure SI 14 A and B) clearly indicate an inverse hexagonal morphology. Second, the Keggin source was changed to H_3PW resulting in inverse hexagonal PB-b-P2VP/H_3PW nanocomposites (Figure SI 14 C and D). Please note, for the latter approach the weight content of H_3PW was adjusted due to the much higher molecular weight of the Keggin unit.

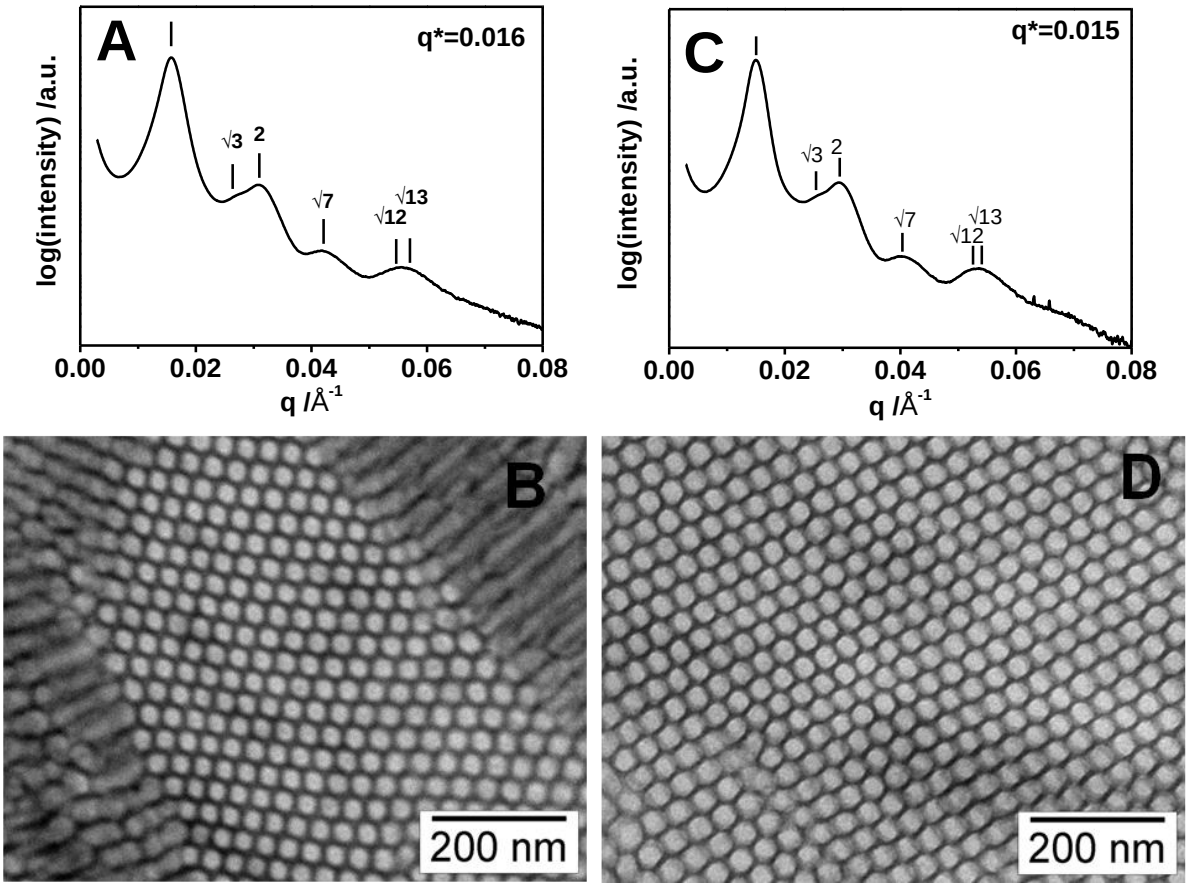

Figure SI 14: Inverse hexagonal mesostructure of PB-b-P2VP/H_3PMo as evidenced by A) SAXS and B) a TEM micrograph obtained from a microtomed film sample. Inverse hexagonal mesostructure of PB-b-P2VP/H_3PW as evidenced by C) SAXS and D) TEM micrograph of a microtomed film sample.

XI. References

(1) Nakamura, O.; Ogino, I.; Kodama, T. *Solid State Ionics* **1981**, *3-4*, 347-351.

(2) Brandrup, J.; Immergut, E. H.; Grulke, E. A. *Polymer Handbook* Wiley: Weinheim, 1999; pp. VI1-VII711.

(3) Rocchiccioliideltcheff, C.; Fournier, M.; Franck, R.; Thouvenot, R. *Inorg. Chem.* **1983**, *22*, 207-216.

(4) Ko, J. H. *Polymer Data Handbook* Oxford University Press: Oxford, 1999; pp. 318-322.

(5) Slim, C.; Tran, Y.; Chehimi, M. M.; Garraud, N.; Roger, J. P.; Combellas, C.; Kanoufi, F. *Chem. Mater.* **2008**, *20*, 6677-6685.

(6) Chen, D.; Xue, Z.; Su, Z. *J. Mol. Catal. A: Chem.* **2003**, *203*, 307-312.

(7) Rocchiccioliideltcheff, C.; Aouissi, A.; Bettahar, M.; Launay, S.; Fournier, M. *J. Catal.* **1996**, *164*, 16-27.